

## Ag buffer layer effect on magnetization reversal of epitaxial Co films

D. H. Wei<sup>1</sup>, C. C. Yu<sup>2</sup>, S. C. Chou<sup>2</sup>, Y. D. Yao<sup>2</sup>, Y. Liou<sup>2</sup>, and T. S. Chin<sup>\*, 1, 3</sup>

<sup>1</sup> Department of Materials Science and Engineering, National Tsing Hua University, HsinChu 300, Taiwan

<sup>2</sup> Institute of Physics, Academia Sinica, Taipei 115, Taiwan

<sup>3</sup> National United University, Miaoli 360, Taiwan

Received 27 June 2004, accepted 2 November 2004

Published online 6 December 2004

PACS 72.15.Gd, 75.50.Cc, 75.60.Jk, 75.70.-i

Nano-sized Ag(111) islands were first prepared by using molecular beam epitaxy technique on diluted-hydrofluoric acid etched Si(111) substrate. Epitaxial Co films were then grown onto the Ag films at 100 °C to decrease interdiffusion. The Ag buffer layer designed to form isolated islands with {111} sidewalls on the Si(111) substrate, and provided Co films (111) texture growth to study the correlation between magnetic properties of Co films and Ag buffer layer effect. It reveals that the Ag rough surface acts as a pinning source and Ag {111} sidewalls also plays an important role on the magnetoresistance transition of Co films.

© 2004 WILEY-VCH Verlag GmbH & Co. KGaA, Weinheim

### 1 Introduction

Various works on the relationship between surface roughness, coercivity and magnetoresistance of thin film and multilayers, have been carried out [1–7]. Very few works have been done on shape effect of a buffer on magnetic properties of film on top [8, 9]. Therefore, it would be interesting to understand the relationship between island-shaped buffer layer and magnetic properties of epitaxial Co films. In a large enough applied magnetic field, the anisotropic magnetoresistance (AMR) measurement will show a change from a positive MR (PMR) value to a negative MR (NMR) value, if we apply a current from parallel to perpendicular the applied magnetic field [10–13]. Nowadays, MR in magnetic films is useful to the applications of large-size memory devices or the magnetic sensor. In this study, we report the use of Ag films grown epitaxially on hydrofluoric acid (DHF) etched Si(111) substrates as templates for the growth of epitaxial Co thin film. So the transition in MR curves and the magnetic properties of Co films under the influence of interface roughness between Co films and Ag buffer layer will be discussed.

### 2 Experiment

Phosphorus-doped Si(111) substrates were cleaned chemically in diluted hydrofluoric acid solution (HF:H<sub>2</sub>O = 1:50) before loading into an ultrahigh vacuum (UHV) chamber. The substrates were first heated to 650 °C outgasing for 1 h. Ag buffer layers in thickness  $t$  nm ( $0 < t < 60$ ) were deposited at 500 °C by a Knudsen cell with deposition rate around 0.05 Å/sec. Then Co (20 nm) film was deposited onto the Ag buffer layer at 100 °C with deposition rate about 0.05 Å/s. The background vacuum was

---

\* Corresponding author: e-mail: ydyao@phys.sinica.edu.tw, Phone: +886-2-27896717, Fax: +886-2-26510530

down to  $6 \times 10^{-10}$  Torr, and the growth pressure was controlled below  $2 \times 10^{-8}$  Torr during deposition. The crystal structure was characterized by *in-situ* reflection high-energy electron diffraction (RHEED). The surface morphology and cross-sectional micrograph were observed by atomic force microscopy (AFM) and transmission electron microscopy (TEM), respectively. The magnetic anisotropy was investigated by angle dependent longitudinal magneto-optical Kerr effect (LMOKE). The magnetoresistive response curves,  $R(H)$ , were measured at 293K by a four-point probe technique with the current  $I$  fixed at 20 mA and the magnetic field  $H$  was applied in the film plane. The rotation angle,  $\varphi$ , is between the direction of the current and the orientation of the applied magnetic field.

### 3 Results and discussion

#### 3.1 Structure identification

Figure 1(a) is the reflection high-energy electron diffraction (RHEED) image of Si(111) surface with the probing e-beam aligned along [100] in-plane direction. The sharp streaks and kikuchi pattern indicate a well define  $7 \times 7$  reconstructed Si(111) surface. Figure 1(b) indicates that the Ag buffer grows epitaxially on the Si(111) substrates. Figure 1(c) and (d) show the RHEED patterns of the Co films grown with and without the 5 nm thick Ag buffer. The Co film grows following patterns of the Ag buffer layer as seen in Fig. 1(c). The investigations of RHEED and TEM patterns show that the main epitaxial relations are Si(111)//Ag(111)//Co(111), and Si[ $\bar{1}10$ ]//Ag[ $\bar{1}10$ ]//Co[ $\bar{1}10$ ]. If the Ag buffer layer was not used, the crystal structure of Co films was polycrystalline as observed in Fig. 1(d).

#### 3.2 Ag buffer layer growth

Due to the constraints of surface energy, the surface energy of Ag ( $1.3 \text{ Jm}^{-2}$ ) is slightly higher than that of Si ( $1.2 \text{ Jm}^{-2}$ ) [14, 15], the buffer Ag film shows island structure as observed by the cross-sectional TEM micrograph shown in Fig. 2(a). The sidewalls of these Ag islands are {111} planes. From above observation indicates that Ag grows on reconstructed Si(111) surface in Volmer-Weber mode. The misfit between the lattice constants of Ag (f.c.c. cubic,  $a = 4.09 \text{ \AA}$ ) and Si (diamond cubic,  $a = 5.43 \text{ \AA}$ ) is  $\sim 24.7\%$ , very close to  $1/4$ , indicates that the Ag atoms grow epitaxially on the Si(111) with 4:3 atomic matching in two-dimensional superlattice. Figure 2(b) and 2(c) show the high-resolution TEM image and election diffraction pattern of Si/Ag interface, respectively. From these observations indicate that Ag unit cells ( $4 \times 4$ ) fits Si unit cells ( $3 \times 3$ ) very well because of the lattice mismatch between Ag cells and Si cells of only 0.4%.

#### 3.3 Magnetic anisotropy

In-plane magnetic anisotropy of Co films was investigated by the longitudinal magneto-optical Kerr effect (LMOKE). The coercivity of the Co films increases linearly as Ag under layer increases, while the squareness value ( $M_r/M_s$ ) decreases with increasing the thickness of Ag buffer layer [16]. The biaxial

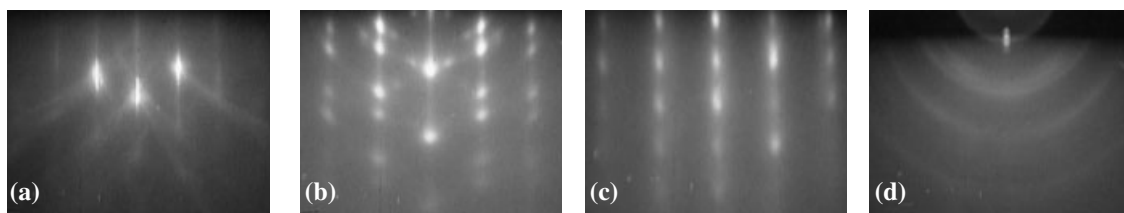


**Fig. 1** RHEED patterns of Si/Ag/Co films with the probing e-beam aligned along the Si[100] in-plane direction; (a) is for Si(111) substrate, (b) is with 5 nm thick Ag buffer on (a), (c) and (d) are RHEED patterns for Co (5 nm) films grown on (b) and (a), respectively.

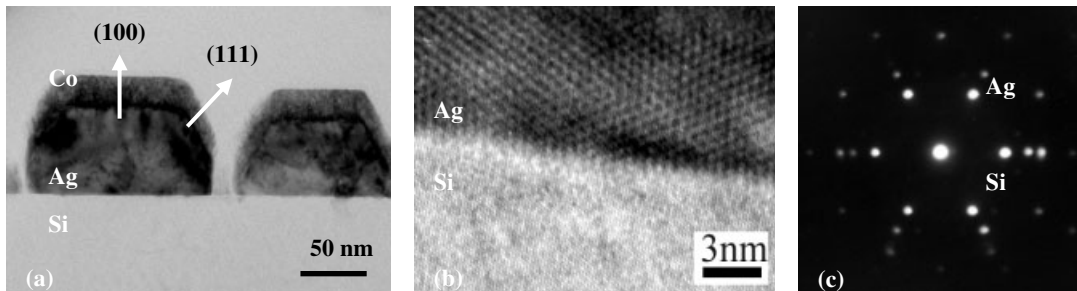


**Fig. 2** Cross-sectional TEM micrograph of the Co films grown on Si(111) substrate with 60 nm thick Ag buffer (a); (b) is HRTEM morphology of Si/Ag interface, and (c) is the electron diffraction pattern corresponding to (b).

magnetic anisotropy without or with a 20 nm thick Ag buffer layer between Si and Co films are depicted in Fig. 3(a) and (b), respectively. When the thickness of Ag buffer is above 20 nm, Co films become magnetically isotropic. Note that the arrows in Fig. 3 indicate the easy-axis directions of Co films. The amplitude of the Co coercivity decreased as the thickness of Ag buffer layer increased. When Ag under layer thickness is over 20 nm, the coercivity value of hard axis is nearly close to easy axis. The surface anisotropy energy density ( $E_{\text{surface}}$ ) is larger than the shape anisotropy energy density ( $E_{\text{shape}}$ ), we expect the origin of anisotropy determined primarily by the crystalline orientation rather than island shape [17]. So the Co films with the biaxial magnetic anisotropy as seen in Fig. 3(a) and 3(b). However, for the Co films grown on the Ag buffer layer that have a thickness greater than 20 nm, the Ag surface roughness induced domain-wall-pinning starts to contribute to the coercivity and shows magnetically isotropic behaviour. The disappearance of biaxial anisotropy could arise from the increase of in-plane demagnetization factor induced by the roughness. From rms roughness of Co films increases linearly with the Ag buffer thickness, it reveals that the Ag rough surface acts as a pinning source.

### 3.4 Magnetoresistance transition

In the MR measurements, two MR peaks are observed in the electrical resistance with  $H$  scanning from the positive direction to the negative, and the reverse direction. Figure 4(a) shows the MR vs  $H$  curves of the Co films on Si(111) substrate without Ag buffer. The angle,  $\varphi$ , represent between the direction of the current and the orientation of the applied magnetic field. The change in the shape of MR loops is clearly seen. If the current is parallel to the field ( $\varphi = 0$ ), the valley shaped MR peaks [called  $P$  (positive) MR]

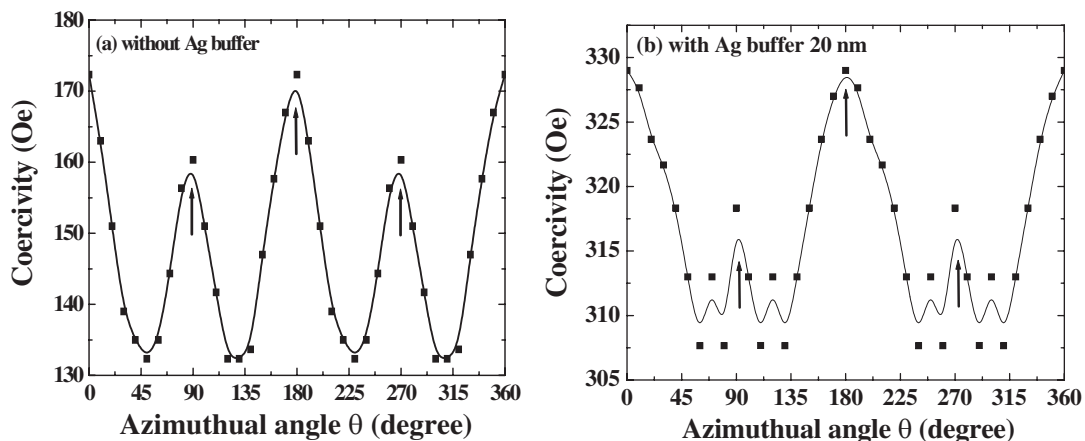


**Fig. 3** Azimuthal distributions of the Co coercivity for (a) without Ag buffer, and (b) with 20 nm thick Ag buffer grown on the Si(111) substrates.

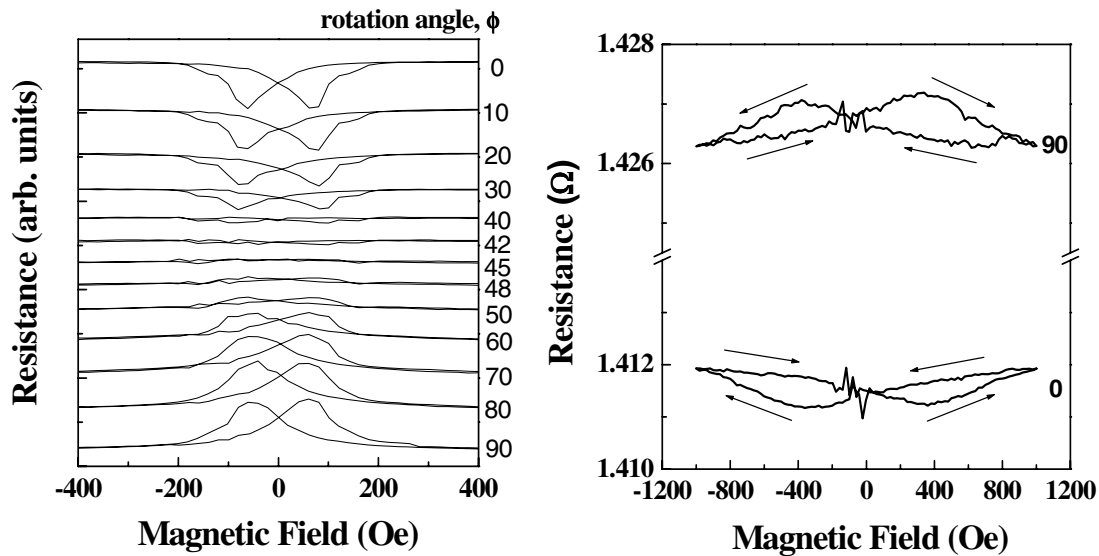


**Fig. 4** MR loops for the Co films grown on Si(111) substrates (a) without, and (b) with 20 nm thick Ag buffer layer. The rotation angle  $\phi$  is between the direction of the current and the orientation of the applied magnetic field.

are observed, while if the current is perpendicular to the field ( $\phi = 90$ ), the bell-jar shaped MR peaks [called  $N$  (negative) MR] are observed. In this case, the components of current parallel and perpendicular to the field are changed according to the rotation of the sample, and the gradual transition from the PMR to NMR behavior can be observed. As the angle  $\phi$  increases, the component of the current perpendicular to the magnetic field is also set in and the NMR part also contributes to the MR peaks. According to the increase of NMR contribution to the MR peaks, the shape of MR peaks is gradually changed. At this range ( $40 \leq \phi \leq 50$ ), both NMR and PMR contribute to the MR peaks at the same time. The negative MR will fully compensate the positive MR and will lead to a straight line. So the MR shape is strongly depended on the rotation angle  $\phi$ . The phenomenon is consistent with the typical AMR. After the formation of Ag islands ( $t \geq 20$  nm) as seen in Fig. 4(b), the sidewalls start to contribute to the MR signal and the resistance value in the  $\phi = 90$  mode is greater than that in  $\phi = 0$  mode. The phenomenon is not typical of AMR. This indicates that the Co film deposited on  $\{111\}$  sidewalls of Ag islands contribute the MR signal of perpendicular component on the magneto-resistance transition.

## 4 Conclusions

We have successfully fabricated epitaxial Ag buffer layer grown on the Si(111) substrates as a template to further deposit Co single layer. The interface roughness between underlying Ag buffer and later grown Co films can be controlled via the thickness control of Ag buffer. The surface and the sidewalls of Ag islands were the key factors for the magnetization reversal of the Co films.

**Acknowledgements** The authors are grateful for the financial supported by National Science Council of ROC under the Grant 91-2120-M-001-004 and NSC92-2120-M-001-008.

## References

- [1] Y. P. Zhao, G. Palasantzas, G. C. Wang, and J. Th. M. De Hosson, *Phys. Rev. B* **60**, 1216 (1999).
- [2] S. P. Li, A. Samad, W. S. Lew, Y. B. Xu, and J. A. C. Bland, *Phys. Rev. B* **61**, 6871 (2000).
- [3] M. Li, Y. P. Zhao, G. C. Wang, and H. G. Min, *J. Appl. Phys.* **83**, 6287 (1998).
- [4] W. Weber, C. H. Back, A. Bischof, Ch. Wursch, and R. Allenspach, *Phys. Rev. Lett.* **76**, 1940 (1996).

- [5] T. L. Monchesky, B. Heinrich, R. Urban, K. Myrtle, M. Klaua, and J. Kirschner, *Phys. Rev. B* **60**, 10242 (1999).
- [6] M. J. Hadley and R. J. Pollard, *J. Appl. Phys.* **92**, 7389 (2002).
- [7] J. V. Kim, M. Demand, M. Hehn, K. Ounadjela, and R. L. Stamps, *Phys. Rev. B* **62**, 6467 (2000).
- [8] C. C. Yu, W. C. Cheng, W. B. Lee, S. Y. Chen, Y. Liou, and Y. D. Yao, *J. Appl. Phys.* **93**, 7468 (2003).
- [9] D. H. Wei, C. C. Yu, S. C. Chou, Y. D. Yao, Y. Liou, and T. S. Chin (unpublished).
- [10] I. Rhee and C. Kim, *Jpn. J. Appl. Phys.* **39**, 6230 (2000).
- [11] J. A. Mendes, V. S. Amaral, J. B. Sousa, L. Thomas, and B. Barbara, *J. Appl. Phys.* **81**, 5208 (1997).
- [12] P. P. Freitas, L. Berger, and J. F. Silvain, *J. Appl. Phys.* **61**, 4385 (1987).
- [13] G. Choe and M. Steinback, *J. Appl. Phys.* **85**, 5777 (1999).
- [14] F. J. Himpsel, J. E. Ortega, G. J. Mankey, and R. F. Willis, *Adv. Phys.* **47**, 511 (1998).
- [15] T. Kawamura, S. Toyoshima, and A. Ichimiya, *Surf. Sci.* **514**, 60 (2002).
- [16] J. Swerts, K. Temst, N. Vandamme, C. Van Haesendonck, and Y. Bruynseraede, *J. Magn. Magn. Mater.* **240**, 380 (2002).
- [17] R. M. H. New, R. F. W. Pease, R. L. White, R. M. Osgood, and K. Babcock, *J. Appl. Phys.* **79**, 5851 (1996).